

# Global Mapping Function (GMF): A new empirical mapping function based on numerical weather model data

J. Boehm,<sup>1</sup> A. Niell,<sup>2</sup> P. Tregoning,<sup>3</sup> and H. Schuh<sup>1</sup>

Received 20 December 2005; revised 23 January 2006; accepted 10 February 2006; published 4 April 2006.

[1] Troposphere mapping functions are used in the analyses of Global Positioning System and Very Long Baseline Interferometry observations to map a priori zenith hydrostatic and wet delays to any elevation angle. Most analysts use the Niell Mapping Function (NMF) whose coefficients are determined from site coordinates and the day of year. Here we present the Global Mapping Function (GMF), based on data from the global ECMWF numerical weather model. The coefficients of the GMF were obtained from an expansion of the Vienna Mapping Function (VMF1) parameters into spherical harmonics on a global grid. Similar to NMF, the values of the coefficients require only the station coordinates and the day of year as input parameters. Compared to the 6-hourly values of the VMF1 a slight degradation in short-term precision occurs using the empirical GMF. However, the regional height biases and annual errors of NMF are significantly reduced with GMF.

**Citation:** Boehm, J., A. Niell, P. Tregoning, and H. Schuh (2006), Global Mapping Function (GMF): A new empirical mapping function based on numerical weather model data, *Geophys. Res. Lett.*, 33, L07304, doi:10.1029/2005GL025546.

## 1. Introduction

[2] For space geodetic measurements, estimates of atmosphere delays are highly correlated with site coordinates and receiver clock biases. Thus it is important to use the most accurate models for the atmosphere delay to reduce errors in the estimates of the other parameters. Numerical Weather Models (NWM) provide the spatial distribution of refractivity throughout the troposphere with high temporal resolution for mapping the zenith troposphere delay to the elevation of each observation by so-called mapping functions. The information needed for the mapping functions must be obtained from an external source, i.e., the NWM, prior to geodetic data analysis. In contrast, the Niell Mapping Function (NMF) was built on one year of radiosonde profiles primarily from the northern hemisphere [Niell, 1996]; the spatial and temporal variability of the mapping function is accounted for with only a latitude and seasonal dependence. This empirical approach considerably simplifies the estimation process since no external data are required. However, following the development of NMF, two deficiencies became evident: a) latitude-dependent biases, which are largest in high southern latitudes, and b) the lack

of sensitivity to the longitude of a site, which causes systematic distortions of estimated positions in some areas, for example over northeast China and Japan. The simple temporal and latitudinal functions of the NMF do not provide the resolution to capture the higher variability in space and time that are seen in mapping functions based on NWM data [Boehm and Schuh, 2004; Boehm et al., 2006].

[3] Boehm et al. [2006] showed from an analysis of Very Long Baseline Interferometry (VLBI) observations that the application of the Vienna Mapping Function (VMF1), with coefficients given at 6-hourly time intervals, considerably improves the precision of geodetic results such as baseline lengths and station heights. VMF1 is currently the mapping function providing globally the most accurate and reliable geodetic results. Moreover, systematic station height changes of up to 10 mm occur when changing from the NMF to the VMF1.

[4] The goal of this paper is to present a mapping function which can be used globally and implemented easily in existing geodetic analysis software and which provides consistency with NWM-based mapping functions, in particular with the VMF1 [Boehm et al., 2006]. The parameterization of the coefficients in the three-term continued fraction (see Equation (1)) that is used in most mapping functions has been refined to include a dependence on longitude. The accuracies of the mapping functions have been improved by extending the temporal range of input data used and also by global sampling of the atmosphere by raytracing through a global NWM instead of the limited number of radiosonde sites used to derive the NMF. The resulting mapping functions, one each for the hydrostatic and wet components, are designated the Global Mapping Function (GMF). In this paper we compare the empirical GMF with mapping functions derived from radiosonde data, with NMF, and with VMF1.

## 2. Mapping Functions

[5] For space geodetic measurements it is convenient to characterize the azimuthally symmetric component of the atmospheric delay by a value in the zenith direction that varies with time on a scale of twenty minutes to a few hours. The delay in the direction of an observation is related to the zenith delay by a mapping function, which is modelled with sufficient accuracy for elevations down to 3° using a three term continued fraction in  $\sin$  (elevation), [Niell, 1996] given by:

$$mf(e) = \frac{1 + \frac{a}{1 + \frac{b}{1 + c}}}{\sin e + \frac{a}{\sin e + \frac{b}{\sin e + c}}} \quad (1)$$

The parameters  $a$ ,  $b$ , and  $c$  are different for the hydrostatic and wet components of the atmosphere, which are

<sup>1</sup>Institute of Geodesy and Geophysics, Vienna, Austria.

<sup>2</sup>MIT Haystack Observatory, Westford, Massachusetts, USA.

<sup>3</sup>Research School of Earth Sciences, Australian National University, Canberra, ACT, Australia.

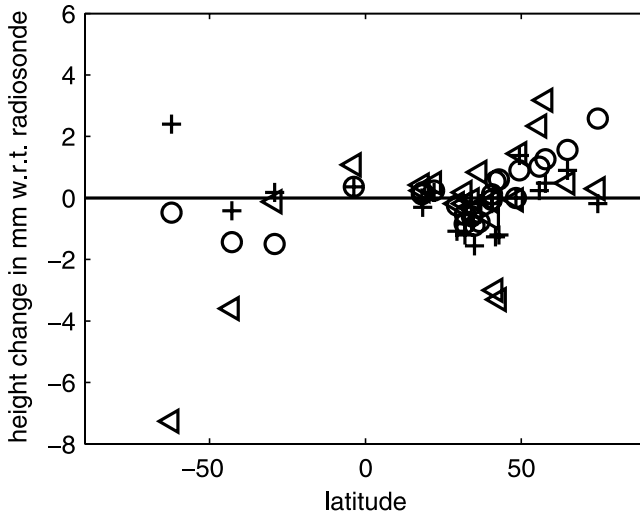


**Figure 1.** Mean height differences in mm for hydrostatic NMF (triangles), GMF (pluses), and VMF1 (circles) relative to radiosonde based mapping functions for 1992.

designated by indices  $h$  or  $w$  in Section 3. They should be related with sufficient accuracy to the characteristics of the atmosphere at the time of observation to avoid introducing significant error into the estimation of the geodetic site coordinates. For NMF [Niell, 1996], each of the parameters is a constant or a function of site latitude (symmetric about the equator) and day of year. Thus, only the seasonal dependence of the temporal variation of the atmosphere is taken into account. The mapping functions IMF [Niell, 2001] and VMF1 [Boehm et al., 2006] use the output of a numerical weather analysis to provide information specifically for the geographic location of the site with a temporal resolution of six hours. They differ in the ease of computation of the parameters and the amount of data used from the NWM. While VMF1 is more accurate, IMF is more generally applicable. The accuracy improvement over NMF is especially significant for the hydrostatic component for both VMF1 and IMF.

[6] Different mapping functions produce different coordinate estimates, not only in terms of precision and repeatability but also with different biases and seasonal variability. It is necessary to use consistent mapping functions for all analyses in order to derive consistent sets of coordinates. The VMF1 is provided only at discrete locations, for example, at all IVS (International VLBI Service for Geodesy and Astrometry) sites and all IGS (International GNSS Service) sites, and does not cover the whole time period of global GPS observations since the early 1990s. Therefore, it is desirable to have a mapping function similar to NMF that can be computed empirically for any site at any date but which is more consistent with the VMF1 than is NMF. Such a mapping function could be seen as a back-up in case the NWM-based models either are not available for some period of time or are discontinued.

### 3. Determination of the Global Mapping Function (GMF)

[7] Using  $15^\circ \times 15^\circ$  global grids of monthly mean profiles for pressure, temperature, and humidity from the

ECMWF (European Centre for Medium-Range Weather Forecasts) 40 years reanalysis data (ERA40), the coefficients  $a_h$  and  $a_w$  were determined for the period September 1999 to August 2002 applying the same strategy that was used for VMF1. Taking empirical equations for  $b$  and  $c$  (from VMF1) the parameters  $a$  were derived by a single raytrace at  $3.3^\circ$  initial elevation angle [Boehm et al., 2006]. Thus, at each of the 312 grid points, 36 monthly values were obtained for the hydrostatic and wet  $a$  parameters. The hydrostatic coefficients were reduced to mean sea level by applying the height correction given by Niell [1996]. The mean values,  $a_0$ , and the annual amplitudes,  $A$ , of a sinusoidal function (Equation (2)) were fitted to the time series of the  $a$  parameters at each grid point, with the phases referred to January 28, corresponding to the NMF. The standard deviations of the monthly values at the single grid points with respect to Equation (2) increase toward higher latitude from the equator, with a maximum value of 8 mm (equivalent station height error) in Siberia. For the wet component, the standard deviations are smaller with maximum values of about 3 mm at the equator.

$$a = a_0 + A \cdot \cos\left(\frac{\text{doy} - 28}{365} \cdot 2\pi\right) \quad (2)$$

$$a_0 = \sum_{n=0}^9 \sum_{m=0}^n P_{nm}(\sin \varphi) \cdot [A_{nm} \cdot \cos(m \cdot \lambda) + B_{nm} \cdot \sin(m \cdot \lambda)] \quad (3)$$

Then, the global grid of the mean values,  $a_0$ , and of the amplitudes,  $A$ , for both the hydrostatic and wet coefficients of the continued fraction form were expanded into spatial spherical harmonic coefficients up to degree and order 9 (according to Equation (3) for  $a_0$ ) in a least-squares adjustment. The residuals of the global grids of  $a_0$  and  $A$  values to the spherical harmonics are in the sub-millimeter range (in terms of station height). The hydrostatic and wet

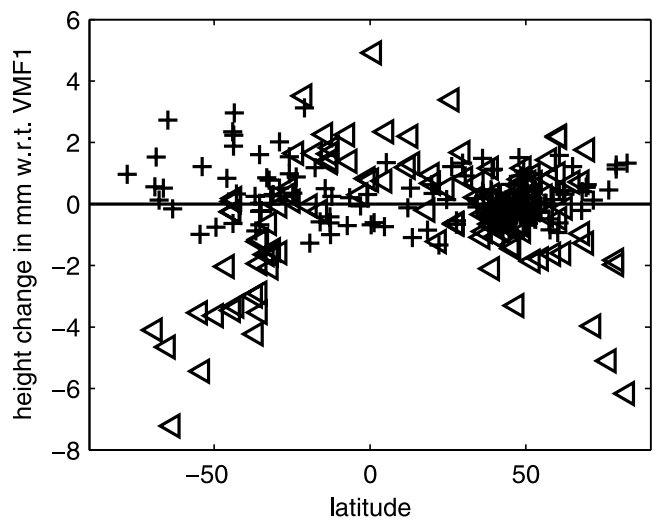


**Figure 2.** Mean height changes in mm when using NMF (triangles) and GMF (pluses) in GPS analysis with heights obtained using the VMF1 as reference.

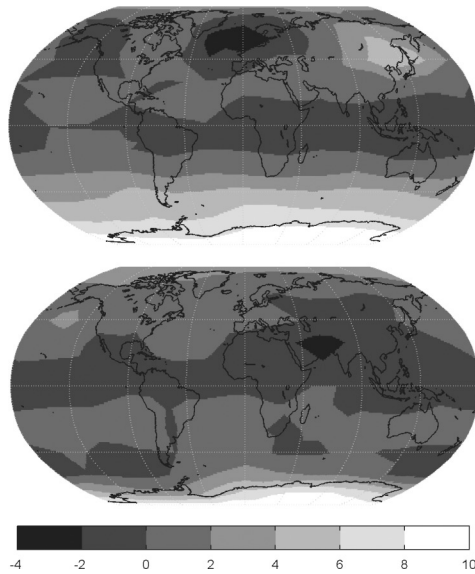


**Figure 3.** Mean height changes (in mm) when using the hydrostatic GMF instead of NMF for (top) January and (bottom) July determined by applying the rule of thumb. The largest differences can be found in January south of  $45^{\circ}\text{S}$  and in northeast China and Japan, with station height differences up to 10 mm.

coefficients  $a$  for any site coordinates and day of year can then be determined using Equation (2).

#### 4. Validation and Comparison of Mapping Functions

##### 4.1. Validation of Mapping Functions By Radiosondes

[8] The most accurate computation of azimuthally symmetric mapping functions is assumed to be obtained from vertical profiles of temperature, pressure, and humidity from radiosondes [Niell *et al.*, 2001]. The mapping function is then computed as the ratio of the delay (obtained by raytracing) along the path at the desired elevation to the delay in the zenith direction. For convenience we compare the mapping functions for a vacuum (outgoing) elevation angle of  $5^{\circ}$ . The radiosonde data used for this comparison are from 23 sites and span the latitude range from  $-66^{\circ}$  to  $+75^{\circ}$ . Although the majority of the radiosonde sites are in the northern hemisphere. A ‘rule of thumb’ [MacMillan and Ma, 1994] states that for azimuthally symmetric delay errors and observations down to approximately  $5^{\circ}$ , the height error is approximately one fifth of the delay error at the lowest elevation. The mapping function differences have been converted to an equivalent height difference using this rule of thumb because station height changes are more easily visualized than differences in the  $a$  coefficients. The mean station height differences, averaged over the year, are shown in Figure 1 after comparing the hydrostatic delays from NMF, GMF, and VMF1 with radiosonde data. The most important feature is the significantly smaller bias for hydrostatic GMF compared to hydrostatic NMF, thus confirming that the mean biases can be reduced with GMF. On the other hand, GMF and NMF are not significantly different

with respect to the standard deviations of the height changes (not shown here) since both contain only annual time variability, whereas the actual variations occur on weekly, daily, and sub-daily time scales. The influence of the wet mapping functions is less critical than the hydrostatic component in GPS and VLBI analyses, since the wet delays are typically smaller than the hydrostatic delays by a factor of 10.

##### 4.2. NMF and GMF Compared to VMF1 in GPS Analysis

[9] A global network of more than 100 GPS stations was analysed with the software package GAMIT Version 10.21 [King and Bock, 2005; Herring, 2005] applying the NMF, GMF, and VMF1 mapping functions. We processed observations from July 2004 through June 2005, producing a fiducial-free global network for each day. The elevation cutoff angle was set to  $7^{\circ}$  and no downweighting of low observations was applied to make the performance of the mapping functions most visible. Atmospheric pressure loading (tidal and non-tidal) [Tregoning and van Dam, 2005] was applied along with ocean tide loading and the IERS2003 solid Earth tide model [McCarthy and Petit, 2004]. We estimated satellite orbital parameters, station coordinates, zenith tropospheric delay parameters every 2 hours, and resolved ambiguities where possible. We used  $\sim 60$  sites to transform the fiducial-free networks into the ITRF2000 by estimating 6-parameter transformations (3 rotations, 3 translations) [Herring, 2005]. For the investigations described below the time series were used of those 133 stations that have more than 300 daily height estimates. The latitudes of the sites are indicated in Figure 2, which shows the mean changes of GPS station

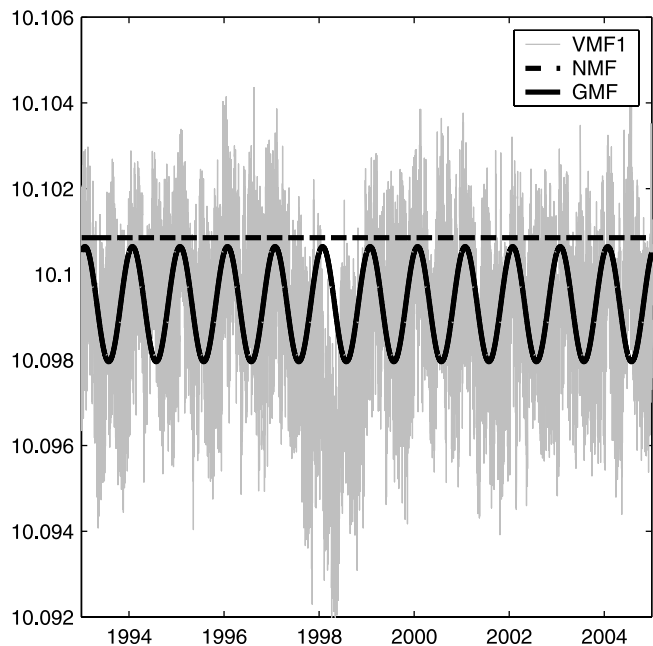


**Figure 4.** Hydrostatic mapping function at  $5^{\circ}$  elevation at Fortaleza, Brazil. Phenomena such as the El Niño event in 1997 and 1998 cannot be accounted for with empirical mapping functions like NMF or GMF that contain only average seasonal terms.

heights with NMF or GMF relative to using VMF1. It is evident that the agreement between VMF1 and GMF is very good, whereas station height differences up to 10 mm occur in the southern hemisphere south of 45°S and in the Japan region when changing from VMF1 to NMF.

#### 4.3. NMF Versus GMF

[10] Computing hydrostatic GMF and NMF for each month on a global grid and applying the rule of thumb, we derived corresponding station height differences. In Figure 3 the height changes from NMF to GMF are plotted for January and July. These comparisons show that there is agreement between NMF and GMF in July (apart from Antarctica), but that in January differences are large (up to 15 mm) south of 45°S and in northeast China and Japan. These height changes vary throughout the year and influence other parameters such as scale and geocenter motion.

[11] In Figure 4 the three hydrostatic mapping functions discussed in this paper are plotted for Fortaleza, Brazil for 5° elevation. The NMF does not show a seasonal variation because this station is situated near the equator (2°S). In contrast, the GMF reflects a seasonal variability and, on average, agrees much better with the VMF1. However, a deficiency is evident in both empirical mapping functions compared to the VMF1 because neither NMF nor GMF reveal the unusual meteorological conditions described by the VMF1 during the El Niño phenomena in 1997 and 1998.

#### 5. Conclusions

[12] To achieve the highest accuracy in VLBI and GPS analyses, it is recommended to use troposphere mapping functions that are based on data from numerical weather models. Today, these mapping functions (e.g., VMF1 [Boehm *et al.*, 2006] or IMF [Niell, 2001]) are available as time series of coefficients with a resolution of six hours. However, for particular time periods or stations where NWM-based mapping functions are not available, the GMF can be used without introducing systematic biases in the coordinate time series, although the short-term precision will suffer. The GMF can serve as a ‘back-up’ mapping function or a compatible empirical representation of the more complex NWM-based mapping functions. The GMF provides better precision than the NMF and smaller height biases with respect to VMF1. It can be implemented

very easily because it uses the same input parameters (station coordinates and day of year) as NMF, which is already implemented in most space geodesy software packages. Code for FORTRAN implementations of VMF1 and GMF are provided at <http://www.hg.tuwien.ac.at/~ecmwf1>, as are the input data for VMF1 and IMF.

[13] **Acknowledgments.** We would like to thank the Zentralanstalt fuer Meteorologie und Geodynamik (ZAMG) for allowing us access to the data of the European Centre for Medium-Range Weather Forecasts (ECMWF). Johannes Boehm and Harald Schuh are grateful to the Austrian Science Fund (FWF) for supporting this work under project P16992-N10. Arthur Niell was supported by NASA contract NNG05HY03C. The GPS analyses were computed on the Terrawulf linux cluster belonging to the Centre for Advanced Data Inference at the Research School of Earth Sciences, The Australian National University.

#### References

- Boehm, J., and H. Schuh (2004), Vienna mapping functions in VLBI analyses, *Geophys. Res. Lett.*, *31*, L01603, doi:10.1029/2003GL018984.
- Boehm, J., B. Werl, and H. Schuh (2006), Troposphere mapping functions for GPS and very long baseline interferometry from European Centre for Medium-Range Weather Forecasts operational analysis data, *J. Geophys. Res.*, *111*, B02406, doi:10.1029/2005JB003629.
- Herring, T. A. (2005), GLOBK global Kalman filter VLBI and GPS analysis program, version 10.1, Mass. Inst. of Technol., Cambridge.
- King, R. W., and Y. Bock (2005), Documentation for the GAMIT GPS processing software release 10.2, Mass. Inst. of Technol., Cambridge.
- MacMillan, D. S., and C. Ma (1994), Evaluation of very long baseline interferometry atmospheric modeling improvements, *J. Geophys. Res.*, *99*, 637–652.
- McCarthy, D. D., and G. Petit (Eds.) (2004), IERS conventions (2003), *IERS Tech. Note 32*, Verl. des Bundesamtes für Kartogr. und Geod., Frankfurt am Main, Germany.
- Niell, A. E. (1996), Global mapping functions for the atmosphere delay at radio wavelengths, *J. Geophys. Res.*, *101*, 3227–3246.
- Niell, A. E. (2001), Preliminary evaluation of atmospheric mapping functions based on numerical weather models, *Phys. Chem. Earth*, *26*, 475–480.
- Niell, A. E., A. J. Coster, F. S. Solheim, V. B. Mendes, P. C. Toor, R. B. Langley, and C. A. Upham (2001), Comparison of measurements of atmospheric wet delay by radiosonde, water vapor radiometer, GPS, and VLBI, *J. Atmos. Oceanic Technol.*, *18*, 830–850.
- Tregoning, P., and T. van Dam (2005), Atmospheric pressure loading corrections applied to GPS data at the observation level, *Geophys. Res. Lett.*, *32*, L22310, doi:10.1029/2005GL024104.
- J. Boehm and H. Schuh, Institute of Geodesy and Geophysics, Gusshausstrasse 27–29, A-1040 Vienna, Austria. (johannes.boehm@tuwien.ac.at)
- A. Niell, MIT Haystack Observatory, Westford, MA 01886, USA.
- P. Tregoning, Research School of Earth Sciences, Australian National University, Canberra, ACT 0200, Australia.